

THE ELECTRON SCATTERING REGION IN SEYFERT NUCLEI

YOSHIAKI TANIGUCHI¹, & NAOHISA ANABUKI^{2,3}

¹Astronomical Institute, Graduate School of Science, Tohoku University, Aramaki, Aoba, Sendai 980-8578, Japan

²Department of Astronomy, Graduate School of Science, The University of Tokyo, 7-3-1 Hongo, Bunkyo, Tokyo 113-0033, Japan

³ISAS, 3-1-1 Yoshinodai, Sagami-hara, Kanagawa 229-8510, Japan

Draft version December 8, 2018

ABSTRACT

The electron scattering region (ESR) is one of important ingredients in Seyfert nuclei because it makes possible to observe the hidden broad line region (hereafter HBLR) in some type 2 Seyfert nuclei (hereafter S2s). However, little is known about its physical and geometrical properties. Using the number ratio of S2s with and without HBLR, we investigate statistically where the ESR is in Seyfert nuclei. Our analysis suggests that the ESR is located at radius between ~ 0.01 pc and ~ 0.1 pc from the central engine. We also discuss a possible origin of the ESR briefly.

Subject headings: galaxies: active - galaxies: Seyfert - galaxies: structures

1. INTRODUCTION

The current unified model of Seyfert nuclei has introduced a dusty torus which surrounds the central engine. Since the torus is considered to be optically very thick, the visibility of the central engine is significantly affected by the viewing angle toward Seyfert nuclei [Antonucci & Miller 1985; Krolik & Begelman 1988; Heisler, Lumsden, & Bailey 1997 (hereafter HLB97); see for a review Antonucci 1993]; i.e., if we observe Seyfert nuclei from favored (unfavored) viewing angles, we can (cannot) see the central engine as well as the broad line region (BLR). This explains why there are two types (type 1 and type 2) of Seyfert nuclei (hereafter S1s and S2s); the orientation of S2s is such that the BLR is obscured from the line of sight. The most important observational evidence for this unified model is the detection of a hidden BLR (HBLR) in the nearby S2, NGC 1068 in optical spectropolarimetry (Antonucci & Miller 1985). Subsequent optical spectropolarimetric observations have detected the HBLR in more than a dozen of S2s [Miller & Goodrich 1990 (hereafter MG90); Tran, Miller, & Kay 1992; Kay 1994; Tran 1995a, 1995b, 1995c; Inglis et al. 1993; Hines & Wills 1993; Young et al. 1996; HLB97]. Although the discovery of the HBLR in the S2s has led to the unified model, the HBLR has been detected in only 20% of the observed S2s (Kay 1994; Tran 1995a). Why do some S2s have the HBLR while the others have no HBLR? This raises a question whether or not all S2s are in fact S1s.

The visibility of the HBLR in S2s may be controlled by the location of the electron scattering region (hereafter the ESR) because the light from the BLR is scattered by free electrons in the ESR and thus comes along our line of sight as the HBLR (Antonucci & Miller 1985; MG90). Therefore, the ESR is one of important ingredients in Seyfert nuclei. Although the nature of the ESR is not clear, the ESR is spatially resolved in the nearby S2, NGC 1068; gaseous blobs with several tens pc are observed up to a radius of $\simeq 300$ pc (Capetti et al. 1995b; see also Kishimoto 1999). Recently, HLB97 made a systematic search for the HBLR for an infrared-selected sample of 16 S2s.

They found that the S2s without HBLR are more reddened in the optical and tend to have steeper infrared colors between $25\ \mu\text{m}$ and $60\ \mu\text{m}$. These findings mean that the S2s without HBLR are viewed from an almost edge-on view toward the dusty torus and thus the ESR is also hidden by the obscuring material. On the other hand, the S2s with HBLR are not so reddened [e.g., $E(B - V) \leq 1$] and tend to have flatter $25\ \mu\text{m}$ -to- $60\ \mu\text{m}$ colors, suggesting that the S2s with HBLR are viewed at an angle intermediate between S1s and S2s without HBLR. In summary, HLB97 adopted the following characteristic radii: < 1 kpc for the NLR, < 300 pc for the ESR, and < 1 pc for the BLR. The characteristic radius of ESR is much larger than that of a typical compact dusty torus, < 1 pc (e.g., Taniguchi & Murayama 1998 and references therein). If all S2s have such extended ESRs and the electron scattering is optically thin, one would find high polarizations above 50% in many S2s (MG90; cf. Wolf & Henning 1999). However, the observed polarizations are usually less than 30% even if the correction for effect of unpolarized featureless continuum is made (e.g., Tran 1995c). Although the spatially extended ESR is observed in NGC 1068, there seems no reason to regard NGC 1068 as a standard S2. There may be a possibility for the majority of S2s that the ESR is hidden by a compact, nuclear dusty torus whose size is < 1 pc. In this Letter, based on this idea, we estimate the typical radial distance of the ESR in Seyfert nuclei and then discuss a possible origin of the ESR. Hereafter, we will refer an S2 with and without the HBLR as S2⁺ and S2⁻, respectively.

2. WHERE IS THE ELECTRON SCATTERING REGION IN SEYFERT NUCLEI?

According to HLB97, it is strongly suggested that the ESR in the S2⁻s is hidden by the obscuring material which is either a dusty torus or more extended dusty matter. Although some Seyfert galaxies such as NGC 1068 have dense gaseous matter in the circumnuclear regions (Tacconi, L. 1998, private communication; Kohno et al. 1996), we assume for simplicity that the obscuring matter is the dusty

torus itself in all S2s. In Figure 1, we show the geometrical relationship between the ESR and the torus adopted in this Letter. Although several dusty torus models for active galactic nuclei (AGNs) have been proposed [Efstathiou & Rowan-Robinson 1990; Pier & Krolik 1992, 1993 (hereafter PK92 and PK93, respectively); Granato & Danese 1994; Granato, Danese, & Franceschini 1997], models of PK92 are quite simple and thus are very useful in investigating statistical properties of dusty tori (PK93; Murayama, Mouri, & Taniguchi 1999). Therefore, we adopt the simple torus models of PK92 who studied the thermally reradiated infrared spectra of the compact dusty tori surrounding the central engine of AGNs by using a two-dimensional radiative transfer algorithm. The torus is a cylinder of dust with a uniform density, characterized by the inner radius (a), the outer radius (b), and the full height (h). A semi-opening angle of the torus is thus given as $\theta_{\text{open}} = \tan^{-1}(2a/h)$.

Given the current unified model of Seyfert nuclei, the number ratio between S1s and S2s can be used to estimate the opening angle of dusty tori from a statistical point of view (e.g., Osterbrock & Shaw 1988; MG90; Lawrence 1991); i.e.,

$$\frac{N(\text{S1})}{N(\text{S1}) + N(\text{S2})} = \Omega/4\pi = 1 - \cos \theta_{\text{open}} \quad (1)$$

where $N(\text{S1})$ and $N(\text{S2})$ are the observed numbers of S1s and S2s, respectively, Ω is the solid angle subtended at the source not covered by dust, and θ_{open} is the semi-opening angle of the torus. Adopting the observed number ratios, $N(\text{S1})/N(\text{S2}) = 0.125$ (Osterbrock & Shaw 1988), 0.20 (Salzer et al. 1989), 0.435 (Huchra & Burg 1992), we obtain $\theta_{\text{open}} \simeq 27^\circ$, 34° , and 46° , respectively. The semi-opening angle derived here is basically quite similar to that of the bi-conical narrow line regions (NLRs) if the NLRs are collimated by the dusty tori (e.g., Murayama et al. 1999). Optical emission-line imaging surveys made by Pogge (1989), Wilson & Tsvetanov (1994), and Schmitt & Kinney (1996) show that a typical semi-opening angle of dusty tori is $\theta_{\text{open}} \simeq 30^\circ$. Accordingly, it seems reasonable to adopt $\theta_{\text{open}} \simeq 30^\circ$ (i.e., $N_{\text{S1}}/N_{\text{S2}} \simeq 0.15$). This means that the viewing angle toward S2s lies in a range between 30° and 90° .

Now let us assume that the S2^+ s are viewed at an angle intermediate between S1s and S2^- s (HLB97). Using the observed number ratio between S2^+ and S2^- , $N(\text{S2}^+)/N(\text{S2}^-)$, together with the observed number of S1s we estimate a semi angle which distinguishes S2^+ from S2^- (θ_{ESR} ; see Figure 1); i.e.,

$$\frac{N(\text{S1}) + N(\text{S2}^+)}{N(\text{S1}) + N(\text{S2})} = 1 - \cos \theta_{\text{ESR}}. \quad (2)$$

There are two surveys for the HBLR in S2s¹. The first survey has been promoted by using the Shane 3 m telescope at Lick Observatory. Ten S2s are known to have the HBLR among 50 S2s studied so far by this survey (Kay 1994; Tran 1995a, 1995c and references therein). Although the S2s are chosen to be brighter than $V = 16$ and have declinations north of -25° , the sample of 50 S2s is not a statistically complete one. It is also noted that the

spectropolarimetry was done in the blue where the signal-to-noise ratio is lower than at $\text{H}\alpha$, making detections of broad $\text{H}\beta$ difficult. Therefore, the detection rate in the Lick survey is regarded as a lower limit. The Lick survey gives an observed number ratio between S2^+ and S2^- , $N(\text{S2}^+)/N(\text{S2}^-) = 0.25 (= 10/40)$. HLB97 made a spectropolarimetric survey for an infrared-selected sample of sixteen S2s at declinations south of $+20^\circ$, with the Galactic latitude $|b| < 20^\circ$, and with high-quality detections at 12, 25, 60, and 100 μm , a 60- μm flux of $f_{60} > 5$ Jy, a far-infrared (FIR) luminosity cutoff of $\log(L_{\text{FIR}}/L_\odot) > 9.85$, and a FIR flux ratio of $f_{60}/f_{25} < 8.5$ to exclude normal spiral galaxies dominated by the cool disk component. They found that seven S2s have the HBLR, giving a ratio of $N(\text{S2}^+)/N(\text{S2}^-) = 0.78 (= 7/9)$. This ratio is higher by a factor of 3 than that obtained in the Lick survey. Although the HLB97 sample seems to be more statistically complete than the Lick one, it includes two ultraluminous infrared galaxies [IRAS 05189–2524 (e.g., Sanders et al. 1988), and IRAS 19254–7245 (Mirabel, Lutz, & Maza 1991)] and one radio-loud AGN (PKS 2048–57 = IC 5063; see, e.g., Simpson, Ward, & Kotilainen 1994). Two (IRAS 05189–2524 and IC 5063) have the HBLR while the other has no HBLR. If we exclude these three galaxies, the number ratio could be 0.63 (5/8). Furthermore, one of their selection criteria, the high-quality detection at 12 μm may reduce the number of S2^- since its mid-infrared emission is usually weak because of the heavy extinction by the torus itself (e.g., PK92). Therefore, we consider that the number ratio derived from the HLB97 sample may be overestimated although the qualitative conclusion in HLB97 is not affected by this possible overestimation.

Using equation (2), we obtain $\theta_{\text{ESR}} \simeq 50^\circ$ for the Lick survey and $\theta_{\text{ESR}} \simeq 80^\circ$ for the HLB97 survey. As mentioned above, the number ratio between S2^+ and S2^- derived from HLB97 survey may be overestimated; note that $\theta_{\text{ESR}} \simeq 65^\circ$ if $N(\text{S2}^+)/N(\text{S2}^-) \simeq 0.5$. Although the Lick S2 sample is not statistically complete, we adopt $\theta_{\text{ESR}} \simeq 50^\circ$ in later discussion keeping the result based on the HLB97 sample in mind. Then one may summarize that the viewing angle toward the S2^+ s lies in the range between 30° and 50° while that toward the S2^- s in the range between 50° and 90° .

Now we can estimate the maximum radial distance of the ESR, r_{ESR} , given the typical dimension of the dusty torus of Seyfert nuclei. Using both dusty torus models of PK92 and high-resolution VLBI imaging data of water vapor maser emission at 22 GHz (Miyoshi et al. 1995; Greenhill et al. 1996, 1997), Taniguchi & Murayama (1998) have shown that the observed inner radii of the water vapor molecular clouds are almost identical to those of dusty tori. Therefore, the inner radii of dusty tori in Seyfert nuclei range from $a \simeq 0.1$ pc (NGC 4258; Miyoshi et al. 1995) to $a \simeq 0.5$ pc (NGC 1068; Greenhill et al. 1996). For the most probable dusty torus model for Seyfert nuclei (PK92, PK93; Murayama et al. 1999), the full height of the torus is $h \simeq 3a$ and thus $h \sim 0.3 - 1.5$ pc. The relation between r_{ESR} and h is given by

$$\frac{r_{\text{ESR}}}{h/2} = \frac{\tan \theta_{\text{ESR}} - \tan \theta_{\text{open}}}{\tan \theta_{\text{ESR}}} \simeq 0.52. \quad (3)$$

¹Note that we do not include the ultraluminous (the infrared luminosity exceeds $10^{12}L_\odot$; see Sanders & Mirabel 1996) type 2 AGNs with the HBLR (see Inglis et al. 1993; Hines & Wills 1993; Young et al. 1996) in our analysis.

We thus obtain $r_{\text{ESR}} \simeq 0.26h \simeq 0.26(h/1 \text{ pc}) \text{ pc}$. Therefore, it is suggested that the ESR is located at radial distance from the central engine, $r_{\text{BLR}} \leq r \leq r_{\text{ESR}}$ where r_{BLR} is the typical radial distance of the BLR; $r_{\text{BLR}} \sim 0.01 \text{ pc}$ (e.g., Peterson 1993). Remember that this argument is basically valid only for a case that the majority of Seyfert nuclei have a compact dusty torus such as those studied by PK92. It is, however, known that some Seyfert galaxies have more spatially extended obscuring clouds (e.g., Kohno et al. 1996). It will be necessary to investigate which type of tori (i.e., compact or extended) is typical for Seyfert nuclei.

Finally, it is worthwhile noting that the viewing angle estimated for the S2⁺s is almost consistent with the lower polarizations, i.e., $P < 30\%$ (MG90; Tran 1995c), even after correcting for probable dilution by the contamination of *unpolarized* featureless continuum emission to the observed spectra (Tran 1995c; see also Heckman et al. 1995; Cid Fernandes & Terlevich 1995; Dopita et al. 1998). If the electron scattering is optically thin, as one expects it to be (cf. Nishiura & Taniguchi 1998), polarizations above 50% would be observed in many S2⁺s (e.g., MG90; cf. Wolf & Henning 1999). It is known that the polarization due to electron scattering depends strongly on the scattering angle (θ_{scat}); e.g., $P \simeq 80\%$ for $\theta_{\text{scat}} \simeq 90^\circ$, $P \simeq 50\%$ for $\theta_{\text{scat}} \simeq 120^\circ$ (or 60°), and $P \simeq 10\% - 15\%$ for $\theta_{\text{scat}} \simeq 150^\circ$ (or 30°) (Kishimoto 1996). Therefore, as suggested in this Letter, if the viewing angle toward the S2⁺s lies in the range between 30° and 50° , the intrinsic polarizations of S2⁺ are expected to be $\simeq 10 - 30\%$ at most, being consistent with the observations. If $r_{\text{ESR}} \geq h/2$, we may not explain the intrinsic lower polarizations in the S2⁺s. This reinforces that our assumption is reasonable; i.e., the radial distance of ESR is shorter than that of the half height of dusty tori (Figure 1).

3. POSSIBLE ORIGIN OF THE ELECTRON SCATTERING REGION

In previous section, we have found that r_{ESR} is of the order of 0.1 pc. In this section we consider possible origins of free electrons in the ESR. There may be two alternative ideas for the origin; 1) free electrons are formed by the photoionization by the ionizing continuum radiation from the central engine, or 2) free electrons are formed by the ionizing shock driven by the radio jet. Recent detailed morphological studies of inner regions of the NLR in some nearby Seyfert nuclei have shown that the optical NLRs are associated with the radio jet (Bower et al. 1995; Capetti et al. 1995a, 1996). These observations have strongly suggested that the NLR associated with the radio jet may be formed by the ionizing fast shock driven by the radio jet rather than the photoionization (Dopita & Sutherland 1995, 1996; Dopita et al. 1997; Bicknell et al. 1998; Falcke, Wilson, & Simpson 1998; Wilson & Raymond 1999; see also Daltabuit & Cox 1972; Wilson & Ulvestad 1983; Norman & Miley 1984). Although it is still uncertain that the majority of the NLR in Seyfert nuclei is formed by the ionizing shock (Laor 1998), the spatial coincidence between the radio jets and the optical emission-line gas means that the ionizing shock works in part. The present analysis has suggested that the ESR is located at $r < 1 \text{ pc}$ from the nucleus. Thus the dynamical effect for the ESR exerted by the radio jet seems much more impor-

tant than that for more distant NLR clouds. Therefore, we investigate the second possibility in this Letter.

Here we consider what happens when a radio jet interacts with the ambient gas following Norman & Miley (1984). The jet is characterized by the jet luminosity L_{jet} , the jet velocity v_{jet} , and the solid opening angle of the jet Ω_{jet} . The pressure exerted on the ambient gas by the radio jet is estimated as

$$p_{\text{jet}} \sim 0.01 \left(\frac{L_{\text{jet}}}{10^{44} \text{ erg s}^{-1}} \right) \left(\frac{\Omega_{\text{jet}}/4\pi}{0.01} \right)^{-1} \left(\frac{r_{\text{jet}}}{1 \text{ pc}} \right)^{-2} \left(\frac{v_{\text{jet}}}{10^5 \text{ km s}^{-1}} \right)^2 \quad (4)$$

where r_{jet} is the radial distance of the jet. If we assume that the ambient gas clouds can cool and reach pressure equilibrium in the cocoon of the jet, we obtain a kinetic temperature of the gas

$$T_{\text{kin}} \sim 10^4 \left(\frac{n_e}{10^{10} \text{ cm}^{-3}} \right)^{-1} \left(\frac{L_{\text{jet}}}{10^{44} \text{ erg s}^{-1}} \right) \left(\frac{\Omega_{\text{jet}}/4\pi}{0.01} \right)^{-1} \left(\frac{r_{\text{jet}}}{1 \text{ pc}} \right)^{-2} \quad (5)$$

where n_e is the electron density. For typical Seyfert nuclei, L_{jet} is of the order of $10^{40} \text{ erg s}^{-1}$ at most (e.g., Wilson, Ward, & Haniff 1988) and v_{jet} is of the order of 10^4 km s^{-1} (e.g., Gallimore, Baum, & O’dea 1996). The typical electron density in the ESR may be closer to that of the inner surface of dusty tori ($\sim 10^8 \text{ cm}^{-3}$; Pier & Voit 1995) than to that in the BLR ($\sim 10^9 \text{ cm}^{-3}$; e.g., Osterbrock 1989). Therefore, we adopt $n_e = 10^8 \text{ cm}^{-3}$ for the ESR (see also Nishiura & Taniguchi 1998). Then we obtain a typical kinetic temperature of the ESR in Seyfert nuclei at $r_{\text{jet}} \sim r_{\text{ESR}} \sim 0.1 \text{ pc}$,

$$T_{\text{kin}}(\text{ESR}) \sim 10^5 \left(\frac{n_e}{10^8 \text{ cm}^{-3}} \right)^{-1} \left(\frac{L_{\text{jet}}}{10^{40} \text{ erg s}^{-1}} \right) \left(\frac{\Omega_{\text{jet}}/4\pi}{0.01} \right)^{-1} \left(\frac{r_{\text{jet}}}{0.1 \text{ pc}} \right)^{-2} \quad (6)$$

As claimed in earlier studies (e.g., MG90), if the electron scattering occurs in a high-temperature gas with $T_{\text{kin}} > 10^6 \text{ K}$, the line width of the HBLR will be broadened thermally; i.e., $\text{FWHM} \simeq 9200(T_{\text{kin}}/10^6 \text{ K})^{1/2} \text{ km s}^{-1}$. However, the observed FWHM of the HBLR lies mostly in a range between $3000 \text{ km s}^{-1} - 6000 \text{ km s}^{-1}$ (MG90; Tran 1995a). Therefore, the above estimate appears consistent with the observations. According to the formulation in equation (6), if $n_e \propto r^{-2}$, the kinetic temperature keeps at $\sim 10^5 \text{ K}$ even for more distant ionized gas clouds. Finding the correlation between FWHM of narrow optical emission lines and their critical densities for collisional deexcitation, De Robertis & Osterbrock (1986) suggested the relation of $n_e \propto r^{-2}$ for S2s (see also Osterbrock 1989, Section, 12.7). This may explain the spatially extended ESRs in NGC 1068. However, even if there are extended ESRs, inner ionized gas clouds will contribute more to the HBLR flux in polarized spectra because their covering factors are larger than those of outer ones if the cloud size is almost similar at any r .

In summary, the thermal Bremsstrahlung emission from this warm gas with $T_{\text{kin}} \sim 10^5 \text{ K}$ can be responsible for the ionization. It is also likely that the jet-driven ionizing shock works there (e.g., Dopita & Sutherland 1995; Falcke et al. 1998; Wilson & Raymond 1999; cf. Laor 1998). The

continuum radiation from these processes may contribute to the so-called featureless continuum emission although dilution by starlight may be important in some S2s. Finally, we would like to mention that the ESR may play an important role in the scattering of X-ray photons (e.g., Turner et al. 1997; Netzer, Turner, & George 1998; Awaki, Ueno, & Taniguchi 1999).

We would like to thank Hisamitsu Awaki and Takashi Murayama for useful discussion and an anonymous referee for useful suggestions and comments. This work was supported in part by the Ministry of Education, Science, Sports and Culture in Japan under Grant Nos. 10044052, and 10304013.

REFERENCES

- Antonucci, R. 1993, *ARA&A*, 31, 473
 Antonucci, R. R. J., & Miller, J. S. 1985, *ApJ*, 297, 621
 Awaki, H., Ueno, S., & Taniguchi, Y. 1999, *Adv. Space Res.*, in press
 Bicknell, G. V., Dopita, M. A., Tsvetanov, Z. I., & Sutherland, R. S. 1998, *ApJ*, 495, 680
 Bower, G. A., Wilson, A. S., Morse, J. A., Geldermann, R., Whittle, M., & Mulchaey, J. S. 1995, *ApJ*, 454, 106
 Capetti, A., Axon, D. J., Macchetto, F., Sparks, W. B., & Boksenberg, A. 1996, *ApJ*, 469, 554
 Capetti, A., Macchetto, F. D., Axon, D. J., Sparks, W. B., & Boksenberg, A. 1995a, *ApJ*, 448, 600
 Capetti, A., Macchetto, F. D., Axon, D. J., Sparks, W. B., & Boksenberg, A. 1995b, *ApJ*, 452, L87
 Cid Fernandes, R. Jr., & Terlevich, R. 1995, *MNRAS*, 272, 423
 Daltabuit, E., & Cox, D. 1972, *ApJ*, 173, L13
 De Robertis, M. M., & Osterbrock, D. E. 1986, *ApJ*, 301, 727
 Dopita, M. A., Heisler, C., Lumsden, S., & Bailey, J. 1998, *ApJ*, 498, 570
 Dopita, M. A., Koratkar, A. P., Allen, M. G., Tsvetanov, Z. I., Ford, H. C., Bicknell, G. V., & Sutherland, R. S. 1997, *ApJ*, 490, 202
 Dopita, M. A., & Sutherland, R. S. 1995, *ApJ*, 455, 468
 Dopita, M. A., & Sutherland, R. S. 1996, *ApJS*, 102, 161
 Efsthathiou, A., & Rowan-Robinson, M. 1990, *MNRAS*, 245, 275
 Falcke, H., Wilson, A. S., & Simpson, C. 1998, *ApJ*, 502, 199
 Gallimore, J. F., Baum, S. A., & O'Dea, C. P. 1996, *ApJ*, 464, 198
 Granato, G. L., & Danese, L. 1994, *MNRAS*, 268, 235
 Granato, G., Danese, L., & Franceschini, A. 1997, *ApJ*, 486, 147
 Greenhill, L. J., Gwinn, C. R., Antonucci, R., & Barvanis, R. 1996, *ApJ*, 472, L21
 Greenhill, L. J., Herrnstein, J. R., Moran, J. M., Menten, K. M., & Velusamy, T. 1997, *ApJ*, 486, L15
 Heckman, T. M., et al. 1995, *ApJ*, 452, 549
 Heisler, C. A., Lumsden, S. L., & Bailey, J. A. 1997, *Nature*, 385, 700 (HLB97)
 Hines, D. C., & Wills, B. J. 1993, *ApJ*, 415, 82
 Huchra, J., & Burg, R. 1992, *ApJ*, 393, 90
 Inglis, M. D., et al. 1993, *MNRAS*, 263, 895
 Kay, L. E. 1994, *ApJ*, 430, 196
 Kishimoto, M. 1996, *ApJ*, 468, 606
 Kishimoto, M. 1999, *ApJ*, in press (astro-ph/9902346)
 Kohno, K., Kawabe, R., Tosaki, T., & Okumura, S. K. 1996, *ApJ*, 461, L29
 Krolik, J. H., & Begelman, M. C. 1988, *ApJ*, 329, 702
 Laor, A. 1998, *ApJ*, 496, L71
 Lawrence, A. 1991, *MNRAS*, 252, 586
 Miller, J. S., & Goodrich, R. W. 1990, *ApJ*, 355, 456 (MG90)
 Mirabel, I. F., Lutz, D., & Maza, J. 1991, *A&A*, 243, 367
 Miyoshi, M., Moran, J., Herrnstein, J., Greenhill, L., Nakai, N., Diamond, P., & Inoue, M. 1995, *Nat*, 373, 127
 Murayama, T., Mouri, H., & Taniguchi, Y. 1999, *ApJ*, submitted
 Netzer, H., Turner, T. J., & George, I. M. 1998, *ApJ*, 504, 608
 Nishiura, S., & Taniguchi, Y. 1998, *ApJ*, 499, 134
 Norman, C., & Miley, G. 1984, *A & A*, 141, 85
 Osterbrock, D. E. 1989, *Astrophysics of Gaseous Nebulae and Active Galactic Nuclei* (San Francisco, Freeman)
 Osterbrock, D. E., & Shaw, R. 1988, *ApJ*, 327, 89
 Peterson, B. M. 1993, *PASP*, 105, 247
 Pier, E. A., & Krolik, J. H. 1992, *ApJ*, 401, 99 (PK92)
 Pier, E. A., & Krolik, J. H. 1993, *ApJ*, 418, 673 (PK93)
 Pier, E. A., & Voit, G. M. 1995, *ApJ*, 450, 628
 Pogge, R. W., 1989, *ApJ*, 345, 730
 Salzer, J. J., Moody, J. W., Rosenberg, J. L., Gregory, S. A., & Newberry, M. V. 1995, *AJ*, 109, 2376
 Sanders, D. B., et al. 1988, *ApJ*, 325, 74
 Sanders, D. B., & Mirabel, I. F. 1996, *ARA & A*, 34, 749
 Schmitt, H. R., & Kinney, A. L. 1996, *ApJ*, 463, 498
 Simpson, C., Ward, M., & Kotilainen, J. 1994, *MNRAS*, 271, 250
 Taniguchi, Y., & Murayama, T. 1998, *ApJ*, 501, L25
 Tran, H. D. 1995a, *ApJ*, 440, 565
 Tran, H. D. 1995b, *ApJ*, 440, 578
 Tran, H. D. 1995c, *ApJ*, 440, 597
 Tran, H. D., Miller, J. S., & Kay, L. E. 1992, *ApJ*, 397, 452
 Turner, T. J., George, I. M., Nandra, K., & Mushotzky, R. F. 1997, *ApJ*, 488, 164
 Wilson, A. S., & Raymond, J. C. 1999, *ApJ*, 513, L115
 Wilson, A. S., & Tsvetanov, Z. I. 1994, *AJ*, 107, 1227
 Wilson, A. S., & Ulvestad, J. S. 1983, *ApJ*, 275, 8
 Wilson, A. S., Ward, M. J., & Haniff, C. A. 1988, *ApJ*, 334, 121
 Wolf, S., & Henning, Th. 1999, *A&A*, 341, 675
 Young, S., et al. 1996, *MNRAS*, 281, 1206

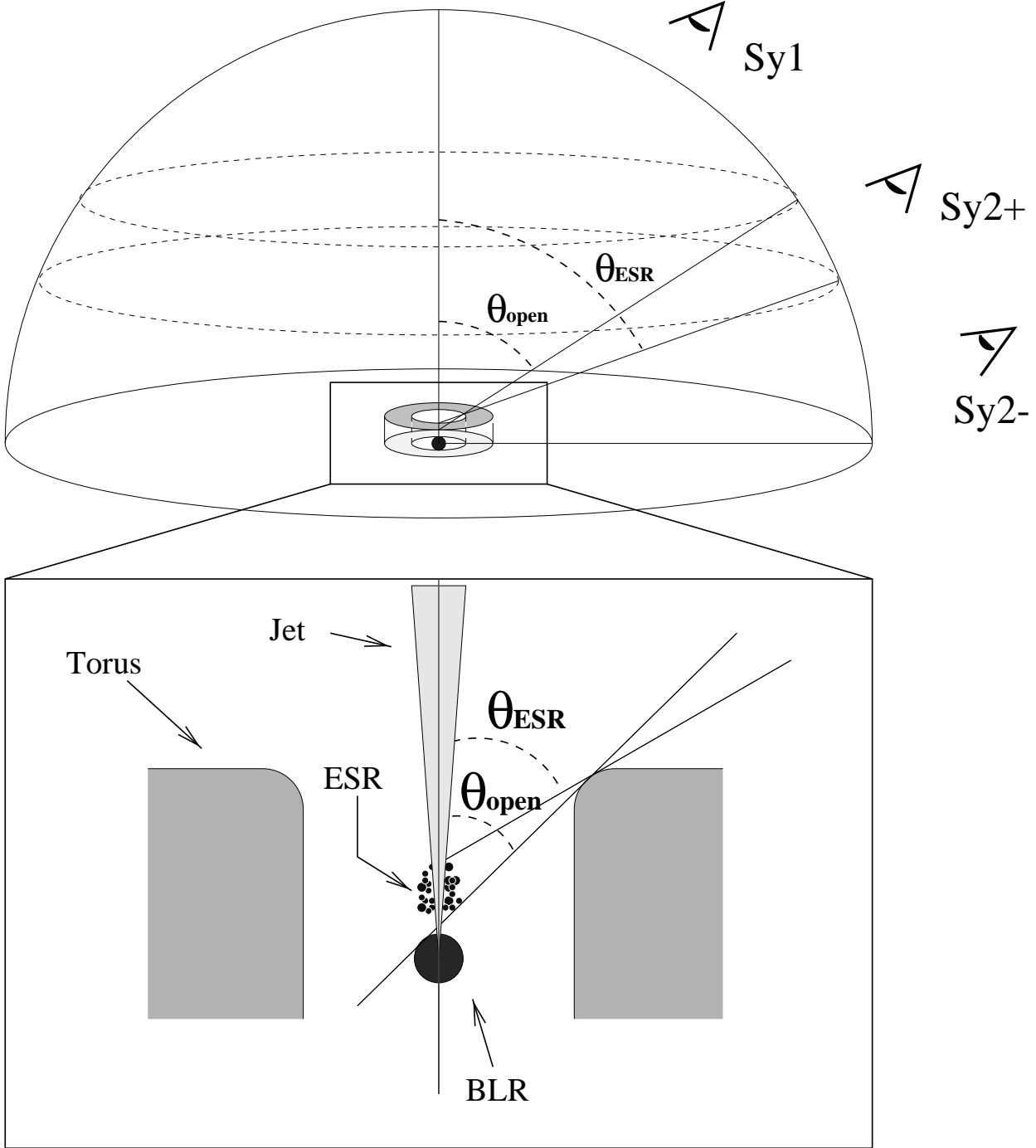


FIG. 1.— A geometrical relationship between the dusty torus and the electron scattering region (ESR).